

Sub-critical regime of femtosecond inscription

Sergei K. Turitsyn¹, Vladimir K. Mezentsev¹, Mykhaylo Dubov¹,
Alexander M. Rubenchik², Michail P. Fedoruk³, and Evgeny V. Podivilov⁴

¹Photonics Research Group, Aston University, Birmingham B4 7ET, UK. (s.k.turitsyn@aston.ac.uk)

²Lawrence Livermore National Laboratory, Livermore, CA 94550, US (rubenchik1@llnl.gov)

³Institute of Computational Technologies, Novosibirsk 630090 Russia (mife@ict.nsc.ru)

⁴Institute of Automation & Electrometry, Novosibirsk 630090 Russia (Podivilov@iae.nsk.su)

Abstract: We apply well known nonlinear diffraction theory governing focusing of a powerful light beam of arbitrary shape in medium with Kerr nonlinearity to the analysis of femtosecond (fs) laser processing of dielectric in sub-critical (input power less than the critical power of self-focusing) regime. Simple analytical expressions are derived for the input beam power and spatial focusing parameter (numerical aperture) that are required for achieving an inscription threshold. Application of non-Gaussian laser beams for better controlled fs inscription at higher powers is also discussed.

©2007 Optical Society of America

OCIS codes: (190.7110) Ultrafast nonlinear optics ; (320.2250) Femtosecond phenomena ; (220.4000) Microstructure fabrication

References and Links

1. K. M. Davis, K. Miura, N. Sugimoto and K. Hirao, "Writing waveguides in glass with a femtosecond. Laser," *Opt. Lett.* **21**, 1729 (1996)
2. E. N. Glezer and E. Mazur, "Ultrafast-laser driven micro-explosions in transparent materials," *Appl. Phys. Lett.* **71**, 882 (1997)
3. D. Homoelle, S. Wielandy, A. L. Gaeta, N. F. Borrelli, and C. Smith, "Infrared photosensitivity in silica glasses exposed to femtosecond laser pulses," *Opt. Lett.* **24**, 1311-1313 (1999)
4. Y. Kondo, K. Nouchi, T. Mitsuyu, M. Watanabe, P. G. Kazansky, and K. Hirao, "Fabrication of long-period fiber gratings by focused irradiation of infrared femtosecond laser pulses," *Opt. Lett.* **24**, 646-648 (1999)
5. A.M. Streltsov and N.M. Borrelli, "Study of femtosecond-laser-written waveguides in glasses," *J. Opt. Soc. Am. B* **19**, 2496-2504 (2002).
6. M. Will, S. Nolte, B. N. Chichkov, and A. Tünnermann, "Optical Properties of Waveguides Fabricated in Fused Silica by Femtosecond Laser Pulses," *Appl. Opt.* **41**, 4360-4364 (2002)
7. R. Osellame, S. Taccheo, M. Marangoni, R. Ramponi, P. Laporta, D. Polli, S. De Silvestri and G. Cerullo, "Femtosecond writing of active optical waveguides with astigmatically shaped beams," *J. Opt. Soc. Am. B*, 1559 (2003)
8. C. Florea and K. A. Winick, "Fabrication and Characterization of Photonic Devices Directly Written in Glass Using Femtosecond Laser Pulses," *IEEE J. Lightwave Technol.* **21**, 246 (2003)
9. B.C. Stuart, M. D. Feit, A. M. Rubenchik, B. W. Shore and M. D. Perry, "Laser-Induced Damage in Dielectrics with Nanosecond to Subpicosecond Pulses," *Phys. Rev. Lett.* **74**, 2248 (1995)
10. B.C. Stuart, M. D. Feit, S. Herman, A. M. Rubenchik, B. W. Shore and M. D. Perry, "Optical ablation by high-power. short-pulse. Lasers," *J. Opt. Soc. Am. B* **13**, 459 (1996)
11. C. B. Schaffer, A. Brodeur, J. F. Garca, and E. Mazur, "Micromachining bulk glass by use of femtosecond laser pulses with nanoJoule energy," *Opt. Lett.* **26**, 93-95 (2001)
12. S. Tzortzakakis, L. Sudrie, M. Franko, B. Prade, A. Mysrowicz, A. Couaeron, and L. Berge, "Self-focusing of few-cycle light pulses in dielectric media," *Phys. Rev. Lett.* **87**, 213902 (2001)
13. 3D Laser Microfabrication: Principles and Applications, Eds. Hiroaki Misawa and Saulius Juodkazis, Wiley-VCH, 2006
14. Q. Feng, J.V. Moloney, A.C. Newell, E.M. Wright, K. Cook, P.K. Kennedy, D.X. Hammer, B.A. Rockwell, C.R. Thompson, "Theory and Simulation on the Threshold of Water Breakdown Induced by Focused Ultrashort Laser Pulses," *IEEE-J. Quantum Electron.* **33**, 127-137 (1997)
15. L.V.Keldysh, "Ionization in the field of a strong electromagnetic wave," *Sov.Phys.JETP* **20**,1307 (1965)
16. M.V.Ammosov,N.V.Delone, and V.P.Krainov "Tunneling ionization of complex atoms and of atomic ions in alternating electromagnetic field," *Sov.Phys.JETP* **64**, 1191 (1986)
17. V. I. Talanov, "Focusing of light in cubic media," *JETP Lett.* **11**, 199 (1970)

18. S.N. Vlasov, V.A. Petrishev, and V.I. Talanov, "Average description of wave beams in linear and nonlinear media," *Izv. Vyssh. Uchebn. Zaved. Radiofiz.* **14**, 1353 (1971) [*Radiophys. and Quantum Electron.* **14**, 1062 (1974)]
 19. R. Y. Chiao, E. Garmire, and C. H. Townes, "Self-trapping of optical beam," *Phys. Rev. Lett.* **13**, 479 (1964)
 20. L. T. Vuong, T. D. Grow, A. Ishaaya, A. L. Gaeta, G.W. 't Hooft, E. R. Eliel, and G. Fibich, "Collapse of Optical Vortices," *Phys. Rev. Lett.*, **96**, 133901 (2006)
-

1. Introduction

Material processing using high-intensity femtosecond (fs) laser pulses is an attractive fast developing technology holding tremendous potential for direct fabrication of multi-dimensional optical structures in transparent media (see e.g. [1-12] and references therein). The technology is based on the induction of an irreversible modification of material (and hence the refractive index) within the focal volume of the laser beam. One of the key attractions of such modification with fs laser pulse is its ability to process non-photosensitive materials. In particular, direct fs inscription in silica is of a specific interest for a wide range of photonic applications. During the writing process multi-photon absorption deposits the energy in the region which can be small compared to the radiation wavelength. The energy of the focused beam/pulse should be small enough not to break the material, but sufficient for the irreversible material modification (it is simply not possible to overview all the relevant recent literature on this subject, therefore, we refer to papers [1-12] and the recent book [13] and references therein). The very process of fs inscription resulting in modification of the refractive index involves a chain of complex phenomena which are not yet fully understood. Due to the important role of multi-photon absorption the laser writing is very sensitive to the field intensity and can be approximately treated as a threshold-like process that starts when the intensity exceeds some critical value I_{th} . For instance, a semi-empirical approach adopted in [7] assumes that the shape of the area with modified refractive index follows the spatial distribution of the generated electron plasma and, effectively, the volume where electric field intensity exceeds a threshold value I_{th} . In other words, because of the sharp dependence of the multi-photon ionisation process on the field intensity, the spatial form of the inscribed structure can be well approximated by resolving an equation on the field intensity: $I(x, y, z) = I_{th}$. This approach, being an obvious simplification, nevertheless, is justified by experimental observations indicating the existence of several different characteristic time scales in the fs laser inscription processes (see [9, 10] for details). At the initial stage, the laser pulse energy is being absorbed by medium through multi-photon absorption followed by impact ionization in cascaded fashion. Both processes create an electron plasma cloud with a shape that follows spatial distribution of light intensity. Next, the energy accumulated in plasma gets transferred to the originally cool solid dielectric during the electron-hole recombination. This process eventually results in irreversible modification of the material density and hence refractive index. However, the latter process takes place during much longer time scale compared with the multi-photon ionization by ultra-short fs pulse. It is assumed that the domain with a modified refractive index that is formed during the second-stage slower processes should reflect an initial shape the electron cloud produced by relatively fast ionization [9,10]. The electron diffusion in such a dense plasma is small and therefore, the spatial distribution of the generated electron plasma can be used as a first simplified approximation of the shape of the inscribed structures [7]. For example, to write the small size structures, waveguides, tightly focused laser light is usually required.

A linear diffraction theory is broadly used to approximately estimate characteristics of a focusing laser beam (see e.g. [7]). Analysis based on the linear diffraction theory leads to an estimate of a spatial pre-focusing of the laser beam (or in other terms, numerical aperture of the focusing lens) required to achieve inscription regime. Note, however, that there is an inherent problem in applying linear diffraction theory to the fs laser inscription analysis. Namely, a rather high intensity (and thus, nonlinearity) should be achieved in the focus and

the multi-photon ionisation leading to modification of the refractive index is essentially nonlinear effect. Indeed, high light intensity required for inscription might affect the laser beam propagation even before ionization and hence energy deposition takes place. One of the important nonlinear phenomena that affects fs laser processing of materials is self-focusing. The self-focusing effect depends on the beam power, and it might modify the laser beam characteristics well before the moment when field intensity will be high enough to engage other nonlinear effects, such as multi-photon absorption. Therefore, it is justified, in the first approximation, to describe effect of the Kerr nonlinearity on the laser beam propagation separately from the other nonlinear effects. Obviously, such a physical assumption has to be verified by analysis of the full model and it will be justified below.

In this work we present a generalization of the linear theory of Gaussian beam focusing to the case of nonlinear propagation solely affected by the Kerr nonlinearity (self-focusing) up until ionization and eventual modification takes place. We re-examine nonlinear diffraction theory in context of fs laser processing of silica in sub-critical (input power less than the critical power of self-focusing) regime. Self-focusing formally lifts restrictions associated with linear propagation such as diffraction limit that is a minimal achievable beam size at the beam waist. It relaxes the need of the tight pre-focusing to inscribe small-size objects and effectively facilitates micro-fabrication of sub-wavelength structures that may correspond to nano-scale structures. It is common to consider the impact of nonlinear effects on the propagation significant only when the laser power is above the critical one for self-focusing. As a matter of fact, it can modify the focal spot for powers below the critical one, and it is one of the aims of this paper to discuss some attractive features of this sub-critical inscription regime. Using powers below critical one can avoid fragmentation and filamentation of the laser beam that is typical for super-critical self-focusing. Therefore, the sub-critical operational regime could be very attractive for microfabrication as more controllable. In particular, this regime can be used to prevent nonlinear beam instabilities and filamentations that can result into inscription of irregular structures.

Typically, the spatial localization of a laser beam is achieved using external focusing by applying lens or similar optical elements. The fs pulse energy required for inscription directly depends on the focusing conditions and can vary from few microJoules (for moderate focusing with 2-3 μm beam waist) to few tens of nanoJoules (for tight focusing to diffraction limit). It has been already understood and experimentally observed that due to high intensity of ultra-short fs pulses the nonlinear index of refraction can affect the beam propagation. Typical average power of fs laser radiation compared to the self-focusing critical power $P_{cr} = 11.68\lambda_0^2 / (8\pi^2 n_0 n_2) = 0.93\lambda_0^2 / (2\pi n_0 n_2)$ can vary in a wide range from sub-critical $P_{in} < P_{cr}$ to super-critical power of $P_{in} \gg P_{cr}$. As it was already pointed out in [2], the beam self-focusing (that starts under condition $P_{in} > P_{cr}$) is unavoidable when the inscription beam is focused into the focal area S_f larger than $S_{cr} = P_{cr} / I_{th}$. Corresponding critical radius is defined as $r_{cr}^2 = P_{cr} / (\pi I_{th})$ is determined by material properties. For silica, the typical value of the critical focal area is approximately about $S_{cr} \approx 14 \mu\text{m}^2$ (e.g. for fused silica at $\lambda_0 = 0.8 \mu\text{m}$, $I_{th} \approx 2.5 \div 3.2 \times 10^{13} \text{ W/cm}^2$ and $P_{cr} \approx 2.3 \text{ MW}$). This condition, evidently, imposes the tough restriction on the produced structure size that should be less than few μm . For some applications, it might be desirable to have inscription in the larger volume while avoiding self-focusing. It is worth to recall that only an input beam with a special nonlinear profile, the so-called Towns mode, experiences self-focusing (collapse of the average beam radius at finite propagation distance) at power $P_{in} = P_{cr}$. For any other laser beam distribution, the critical power required for self-focusing is higher than P_{cr} . It turns out that for the Gaussian input beams the critical self-focusing power P_{cr_G} is, indeed, very close to P_{cr} :

$P_{cr_G} = \lambda_0^2 / (2\pi n_0 n_2) \approx P_{cr}$. We would like to point out, however, that for non-Gaussian laser beam with powers higher than the critical the self-focusing can be rather different compared to Gaussian-like beams. At the first stage of the evolution of the non-Gaussian beam, it will not collapse straightforward, but depending on the initial geometry sooner or later will evolve to some spatial distribution where self-focusing spikes that engage exactly P_{cr} can be formed. Practically this means that self-focusing of a non-Gaussian beam can be delayed (in space) even at powers higher than P_{cr} opening a way to make direct inscription in focal areas larger than $S_{cr} = P_{cr} / I_{th}$ that could be of interest for telecom applications. Taking into account a finite interaction distance of the fs laser pulse and material, application of non-Gaussian beams can provide new interesting regimes of inscription. We propose here to use non-Gaussian laser beams with a critical power well above of $P_{cr_G} \approx P_{cr}$ to achieve modification of the refractive index in a larger spot area. Below we present a particular example of such laser beams that can be either generated using non-fundamental laser modes or created by applying additional optical elements. We also review a theory of the sub-critical inscription regime and quantify the interplay between linear focusing (using the optical lens) and nonlinear self-focusing that relaxes some restrictions imposed in the linear regime.

2. The model and basic equations

The local material modification in the regime of low repetition rate radiation is caused by a single pulse. The modification of the dielectric medium is initiated by the transfer of the pulse energy to the free electrons with the corresponding mapping of the deposited energy distribution into the geometric characteristics of the modified material volume. Evolution of the electric field envelope $A(\vec{r}_\perp, z, t)$ is governed by the nonlinear partial differential equations that accounts for the major propagation effects such as diffraction, Kerr nonlinearity, group velocity dispersion, multi-photon absorption, impact ionization and absorption and defocusing by the generated electron plasma (see e.g. [7,10,12,14]):

$$(1a) \quad iA_z + \frac{1}{2k} \nabla_\perp^2 A - \frac{k''}{2} A_{tt} + k_0 n_2 |A|^2 A = -\frac{i\sigma}{2} (1 + i\omega\tau_e) \rho A - \frac{\beta^{(K)}}{2} |A|^{2K-2} A$$

$$(1b) \quad \rho_t = \frac{1}{n_b^2} \frac{\sigma_{bs}}{E_g} \rho |A|^2 + \frac{\beta^{(K)}}{K\hbar\omega} |A|^{2K}$$

The last three terms in the left-hand side of Eq.(1a) describe effects of beam diffraction, group velocity dispersion (GVD), and Kerr nonlinearity, respectively. The latter is responsible for a catastrophic self-focusing which is limited by the effects described by terms on the right-hand side of Eqs. (1), namely plasma absorption and multi-photon absorption. In Eq.(1a) the laser beam propagation along the z axis is assumed and this equation is essentially a reduced paraxial approximation of the wave equation for the complex electric field envelope A with a carrier frequency ω in the moving frame of coordinates. Here $k = n_b k_0 = n_b \omega / c$ is the propagation vector, n_b is the linear refraction index of silica, k'' is the GVD parameter, n_2 is the nonlinear coefficient, σ_{bs} is the cross section for inverse Bremsstrahlung, τ_e is the electron relaxation time, and the quantity β_K describes the K -photon absorption. Eq.(1b) implements the Drude model for electron-hole plasma in the bulk of silica and describes the evolution of the electron density ρ . The first term on the right-hand of Eq.(1b) side is responsible for the avalanche impact ionization and the second term — for the ionization resulting from multi-photon absorption (MPA). The expression for the multiphoton ionization is a good fit of the general Keldysh expression [15] for ionisation in strong field for not very high intensities. For fused silica and 1 μ m light the intensity must be below 1000 TW/cm². For

higher intensities tunnelling through the binding barrier takes place during the time shorter than the laser period. In this case in Eq.(1.b) one must use the expression for ADK tunnelling ionization [16]. For the problem of inscription the results are not sensitive to the details of field induced ionization [10]. Eq.(1b) is suitable for description of the sub-picosecond laser pulses when energy transfer to the lattice and plasma diffusion is negligible. The model (1) can be considered as a generalization of the nonlinear Schrödinger equation (NLSE). Note that in most of situations of interest, the higher-order nonlinear terms in this model contribute to the fine dynamics of the self-focusing (wave collapse) arrest, while the initial stage of beam propagation is mainly governed by only two effects: *diffraction* and *Kerr nonlinearity*.

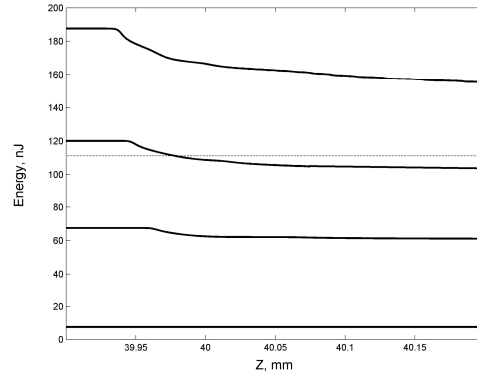


Fig. 1. Evolution of the pulse energy with distance for different input peak powers. Horizontal dashed line corresponds to the critical power for a given initial Gaussian pulse width (FWHM) of 70 fs.

Figure 1 illustrates that at the initial stage of the evolution the pulse energy is conserved. Some simple estimates show that during this stage of the propagation the evolution with a good accuracy is governed by the NLSE. It is also seen that in sub-critical regime the energy transfer to the material can be realised in a sharper manner compared to regimes with pulse power above critical. In the numerical example shown in Fig. 1, the following Gaussian pulse/beam has been used

$$A(r,0,t) = \sqrt{\frac{E_{in}}{\pi\sqrt{\pi}\tau a_s^2}} \exp\left[-\frac{(1+iC_s)r^2}{2a_s^2} - \frac{t^2}{2\tau^2}\right],$$

where $a_s = 1.77$ mm, $\tau = 42$ fs and $C_s = 892$ (this corresponds to the focusing lens with $f = 40$ mm, recalculated using relation $C_s = a_s^2 k / f$). Here the index s stands for surface, indicating that these are the beam characteristics at the surface of a dielectric, after propagation of a distance d from lens to the surface. Note that depending on the distance to the surface and initial pre-focusing conditions, the field distribution at the surface of a dielectric can be rather different from the initial beam parameters. The dashed line in Fig. 1 is for the critical energy of 116 nJ that corresponds to the input pulse with the width of about 70 fs and the critical power of 2.3 MW (in fused silica with $n_b = 1.453$ and $n_2 = 3.2 \times 10^{-16}$ cm²/W). We considered the laser wavelength λ_0 to be 800 nm, and the other parameters for fused silica, used in simulations are: $k'' = 361$ fs²/cm, $\tau_e = 1$ fs, inverse Bremsstrahlung cross section

$\sigma_{bs} = 2.78 \times 10^{-18}$ cm². Multiphoton absorption coefficient $\alpha_K = \beta^{(K)} h\nu \sigma_K \rho_{at}$, where $\rho_{at} = 2.1 \times 10^{22}$ atoms/cm³ is a material concentration and $\sigma_K = 1.3 \times 10^{-55}$ cm^{2K}/W^K/s. We assume here for fused silica a five-photon ionization with $K=5$ and $E_g = 7.6$ eV.

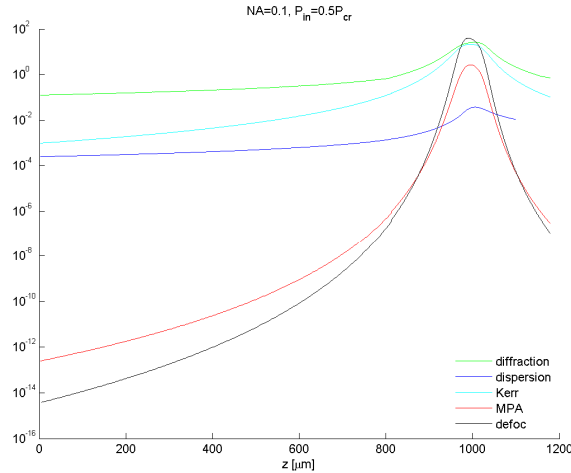


Fig. 2. Relative role of different physical effects (Eqs (1)) in the process of fs laser radiation interaction with silica. Here the input power $P_{in} = 0.5P_{cr}$ and the numerical aperture NA=0.1.

Figure 2 shows relative contributions of different terms in Eqs. (1) in the process of interaction of fs laser radiation with silica medium. The dimensionless focusing parameter C_s was about 25 in these calculations and initial beam radius at the surface a_s was nearly $70 \mu\text{m}$. All other parameters including material parameters are the same as for Figure 1. It is seen that apart from the narrow region where plasma defocusing and multi-photon absorption come into play, the electric field evolution during noticeable interval is mostly affected by the two physical effects: linear diffraction and the Kerr nonlinearity. While linear diffraction dominates initial propagation stage, the Kerr nonlinearity has an impact on the field dynamics as the pulse approaches a focal point that is getting stronger as pulse approaches the energy deposition region. The Kerr nonlinearity acts as a nonlinear lens [17] producing corresponding deformations of the beam waveform. The aim of this paper is to present simple theoretical methods to account for such deformations.

Note that when the high order nonlinear ionization dominates, the absorption can be well approximated by a hard threshold (step-function) process. In other words, this approximation means that the part of the pulse energy is absorbed (transferred to free electrons) when the intensity $I = |A(\vec{r}_\perp, z, t)|^2$ exceeds the threshold I_{th} , leading to consecutive medium modification mapping the corresponding spatial distribution of the intensity into the refractive index changes. In what follows we assume that at $z = 0$ pre-focused laser beam (pulse in time) with a time-spatial waveform $A(\vec{r}_\perp, z = 0, t) = A_0(\vec{r}_\perp, t)$ enters the dielectric medium (e.g. silica). Evolution of the powerful laser beam at first stage is described by the interplay between two focusing mechanisms: linear focusing, due to the lens, and nonlinear self-focusing. Note that typically, pre-focusing lens is used at some distance of the silica, and the boundary conditions $A_0(\vec{r}_\perp, t)$ should be understood correspondingly.

3. Sub-critical self-focusing regime

Next we demonstrate that analysis of the simplified, yet reasonable model based on the NLSE can provide important characteristics of the sub-critical inscription regime. The theory presented below is a simple generalisation of the broadly used linear focusing theory by the nonlinear Kerr effect for the beam power below self-focusing threshold. Evolution of the transversal root-mean-square width of the laser beam within the framework of the NLSE

model is given by the well-known analytical expression derived by Vlasov, Petrishev and Talanov in [18] for the root-mean-square (RMS) of the laser beam:

$$R^2(z) = \frac{\int_{\vec{r}_\perp}^2 |A|^2 d\vec{r}_\perp}{\int |A|^2 d\vec{r}_\perp} = C_1 z^2 + C_2 z + R^2(0), \quad \text{where } z\text{-independent } C_1, C_2 \text{ are determined}$$

by the parameters of the incident beam ($P = \int |A_0|^2 d\vec{r}_\perp$ is the instantaneous input power) and focusing conditions

$$C_1 = \frac{\lambda_0^2}{4\pi^2 n_0^2} \frac{\int |\vec{\nabla}_\perp A_0|^2 d\vec{r}_\perp}{P} - \frac{n_2}{n_0} \frac{\int |A_0|^4 d\vec{r}_\perp}{P}, \quad C_2 = \frac{\lambda_0}{\pi n_0} \frac{\int (\vec{r}_\perp \cdot \vec{\nabla}_\perp \arg(A_0)) |A_0|^2 d\vec{r}_\perp}{P}.$$

We would like to point out that this well-known result is very general and no assumption about the beam shape has yet been made. Substitution of the particular input beam distribution leads to the analytical description of the beam focusing in terms of RMS characteristics. Now, without loss of generality, we illustrate the general result, considering several particular examples of the input laser beam distributions. We would like to stress that this approach can be applied to a variety of spatial beam forms.

3.1. Sub-critical focusing of the Gaussian-shape pulses

First, we describe achieving inscription period with the most widely used pre-focused Gaussian input pulse $A(r,0,t) = \sqrt{\frac{E_{in}}{\pi\sqrt{\pi}\tau a_s^2}} \exp[-\frac{(1+iC_s)r^2}{2a_s^2} - \frac{t^2}{2\tau^2}]$. Here a_s is a beam width parameter. The focusing conditions at the surface are combined in a single focusing parameter $C_s = \pi(f-d)NA^2 / [\lambda(1-NA^2)]$ which is expressed through lens focal distance f , numerical aperture NA and the distance d from lens to the surface. In the case of the Gaussian laser beam, the nonlinear evolution of the RMS beam radius is given by the following equation (that we present for convenience of the comparison in the form similar to the linear focusing theory):

$$(2) \quad R^2(z,t) = R_{\min_NL}^2 \left(1 + \frac{(z - z_{\min_NL})^2}{Z_{R_NL}^2}\right),$$

$$R_{\min_NL}^2 = \frac{a_s^2 [1 - \frac{P(t)}{P_{cr_G}}]}{1 + C_s^2 - \frac{P(t)}{P_{cr_G}}}, \quad Z_{R_NL}^2 = \frac{k^2 a_s^4 [1 - \frac{P(t)}{P_{cr_G}}]}{[1 + C_s^2 - \frac{P(t)}{P_{cr_G}}]^2}, \quad z_{\min_NL} = \frac{k a_s^2 C_s}{[1 + C_s^2 - \frac{P(t)}{P_{cr_G}}]}.$$

Here $P = \int |A_0|^2 d\vec{r}_\perp = \frac{E_{in}}{\tau\sqrt{\pi}} \exp[-\frac{t^2}{\tau^2}] = P_{in} \exp[-\frac{t^2}{\tau^2}]$ and $P_{cr_G} = \lambda_0^2 / (2\pi n_0 n_2)$ is the

critical power of self-focusing for the Gaussian beams, and $k = 2\pi n_0 / \lambda_0$. This equation generalizes the usual linear focusing conditions to the nonlinear (sub-critical $P < P_{cr_G}$) case.

The minimal beam radius $R_{\min} = a_s (1 - P/P_{cr_G})^{1/2} / (1 + C_s^2 - P/P_{cr_G})^{1/2}$ is achieved at the distance z_{\min_NL} . The nonlinear lens allows for better control of the beam energy deposition. The important new feature is that the nonlinearity removes the restriction of the linear focusing, such as the existence of the minimal beam radius that can be achieved under the

fixed pre-focusing C_s . Another interesting feature is that using regimes with small enough effective C_s , it could be possible to change by varying input power the ratio of the beam focal diameter $d_{\min} = 2R_{\min}$ to the confocal parameter $b = 2Z_{R_NL}$ - a nonlinear lens analog of the linear astigmatic beam approach used in [7]. Note, however, that nonlinear astigmatism works only in one direction – making the longitudinal size of the modified area even more lengthy compared to the transversal diameter. This can be useful in writing waveguides along the z-axis.

Considered approach provides an exact analytical description (Eq. 2) of the nonlinear evolution of the root-mean-square beam diameter for arbitrary input beam profile. However, as it was discussed above, the shape of the modified material volume is correlated with the local field characteristic –spatial distribution of the intensity $I(x,y,z)$. Thus, the next important issue is to describe spatial areas where intensity exceeds the inscription threshold value. Provided that a laser beam preserves a one-scale (for instance, Gaussian-like form) field distribution during the focusing it would be possible to determine the intensity distribution. Taking into account a conservation of the power during propagation regime dominated by Kerr nonlinearity, one can estimate intensity as $I = P/S \approx P/(\pi R^2)$. It is convenient to introduce the initial beam spot area S_s defined through $P_{in} = I_s \times S_s = I_s \times \pi a_s^2$. The intensity reaches its maximum at the $z = z_{\min}$ at the time $t = 0$ (in moving frame). Thus, in this case, the necessary condition on the input pulse parameters to provide the intensity above the inscription threshold would be:

$$I_{th} = \frac{P_{in}}{\pi R_{\min}^2} = \frac{P_{in} [1 + C_s^2 - \frac{P_{in}}{P_{cr}}]}{S_s [1 - \frac{P_{in}}{P_{cr}}]}$$

Resolving this equation one would estimate the minimal input power required to initiate inscription:

$$(3) \quad \frac{P_{in}}{P_{cr}} = \frac{1}{2} \left\{ 1 + C_s^2 + \frac{I_{th} S_s}{P_{cr}} - \sqrt{\left[1 + C_s^2 + \frac{I_{th} S_s}{P_{cr}} \right]^2 - \frac{4 I_{th} S_s}{P_{cr}}} \right\}$$

In the case of a tight focusing, typically a condition $P_{in}/P_{cr} \ll (1 + C_s^2)$ is satisfied on the dielectric surface, and the expression (3) can be further simplified (compare with [11]):

$$(3b) \quad \frac{E_{in}}{\tau \sqrt{\pi}} = P_{in} \approx \frac{I_{th} S_s}{(1 + C_s^2) + I_{th} S_s / P_{cr}}, \quad \frac{P_{in}}{P_{cr}} \ll (1 + C_s^2)$$

However, this simple consideration, unfortunately, does not work for powers approaching the critical power. Above estimate is based, indeed, on a very strong assumption — a shape preserving evolution, that is actually not correct for beam powers close to the critical one. This is illustrated by Figure 3 where a normalised product of the maximum of the field intensity and the minimal RMS beam width at the nonlinear focal point is shown as a function of the input beam power for different focusing parameters. Evolution of the input Gaussian beams with $a_s = 100 \mu m$, different input powers and spatial focusing parameters C_s has been computed in the framework of the NLSE model. It is seen that a simple approximation $I_{\max} \times R_{RMS_min}^2 \approx P_{in} / \pi$ (dashed line in Fig. 3) works rather well for the input beam powers up to half of a critical power $P_{in} \leq 0.5 \times P_{cr}$. However, for the input powers in the interval $0.5 \times P_{cr} \leq P_{in} < P_{cr}$ the dependence is more complicated and this is correlated with the fact

that field distribution at the focal point evolves toward the so-called Townes mode [19] from initial Gaussian in this power region. Figure 3 shows that still there is a generic formula linking maximum of intensity and the minimal RMS beam width:

$$(4) \quad I_{th} = \frac{P_{cr}}{\pi R_{min}^2} \times f\left(\frac{P_{in}}{P_{cr}}\right) = \frac{P_{cr} \times [1 + C_s^2 - \frac{P_{in}}{P_{cr}}]}{S_s \times [1 - \frac{P_{in}}{P_{cr}}]} \times f\left(\frac{P_{in}}{P_{cr}}\right) \approx \frac{P_{cr} \times [1 + C_s^2]}{S_s \times [1 - \frac{P_{in}}{P_{cr}}]} \times f\left(\frac{P_{in}}{P_{cr}}\right),$$

Here function $f(x)$ is plotted and numerically approximated in Fig. 3. We would like to point out that this estimate of the maximal intensity does not depend on the initial pulse focusing as can be seen in Fig. 3.

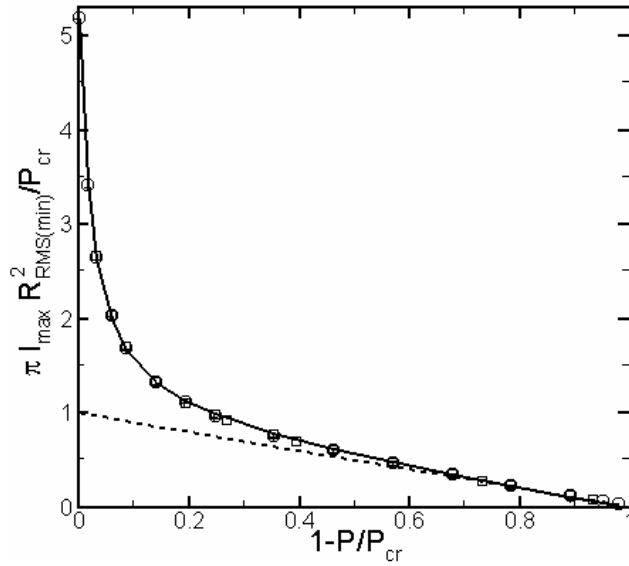


Fig. 3. Product of the maximum field intensity and minimal RMS beam width vs input beam power. The dashed line corresponds to assumption $I_{max} \times R_{RMS_min}^2 \approx P_{in} / \pi$, the markers are results of numerical simulation of 2d NLSE: the circles- $C_s = 25$, the crosses- $C_s = 50$, the squares- $C_s = 100$. The solid line is an approximation by the method of the least squares (here $x = P_{in} / P_{cr}$):

$$f(x) = -1.0073 \times (1.01 - x) + 0.91445 + 8.567 \cdot 10^{-2} / (1.01 - x) - 4.273 \cdot 10^{-4} / (1.01 - x)^2$$

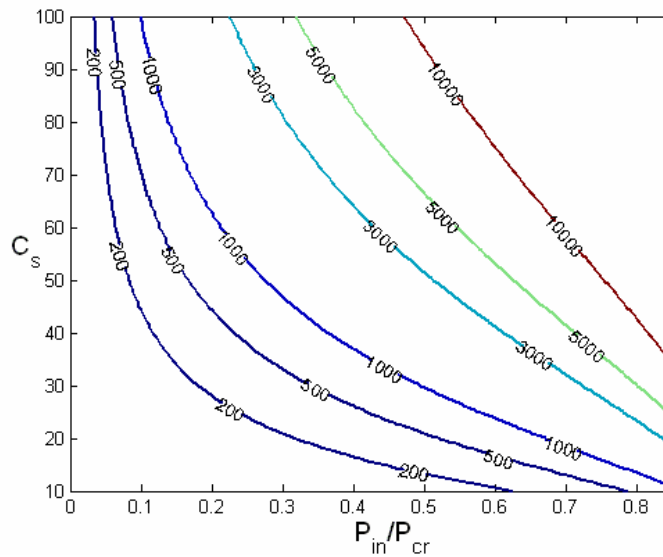
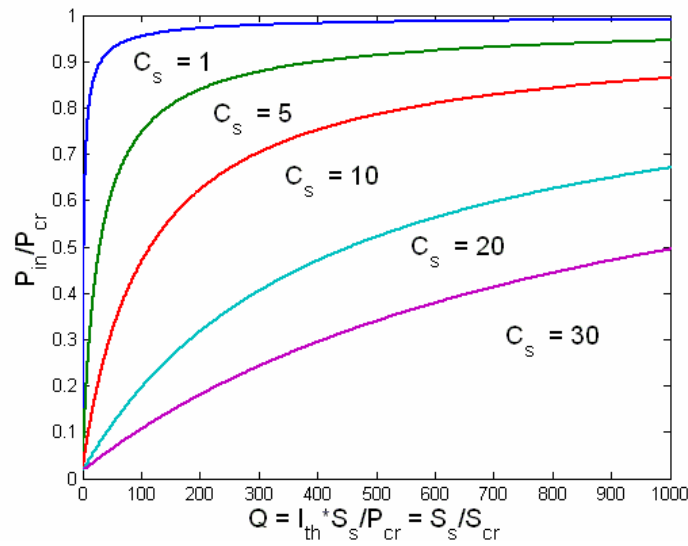


Fig. 4. Numerical solutions of the Eq. 4. Top: Input pulse power (measured in critical power) required to produce intensity above the threshold of inscription is shown as a function of the parameter $Q = I_{th} \times S_s / P_{cr} = S_s / S_{cr}$ – ratio of the beam spot area at the surface to the “critical” focal area $S_{cr} = P_{cr} / I_{th}$ for different pre-focusing parameters C_s . Bottom picture: isolines of the parameter Q in the plane $(C_s, P_{in} / P_{cr})$.

Resolving the transcendent Eq. 4 against input power we get a more accurate (compared to Eq. 3b) estimate of the minimal input power required for inscription:

$$\frac{P_{in}}{P_{cr}} = \tilde{g}\left(C_s^2, \frac{I_{th} S_s}{P_{cr}}\right) \approx g\left(\frac{I_{th} S_s}{P_{cr}(1+C_s^2)}\right).$$

Here function $g(x)$ with $x = \frac{I_{th} S_s}{P_{cr}(1+C_s^2)} \equiv \frac{Q}{(1+C_s^2)}$ is easily found by resolving Eq. 4 and is plotted in Figure 4 for several values of C_s .

Note that instead of analysis of the nonlinear evolution of the field A with pre-focusing condition:

$$A(z=0, \vec{r}) = A_0(\vec{r}) \exp\left[-\frac{i C_s r^2}{2 a_s^2}\right],$$

as it was pointed out in [17], it is enough to find a solution of the NLS equation $U(x,y,z)$ with the non-focused initial beam profile: $U(z=0, \vec{r}) = A_0(\vec{r})$. Then the evolution of the pre-focused beam $A(x,y,z)$ is found using the Talanov's (lens) transform [17] as:

$$A(z, \vec{r}) = \frac{1}{L(z)} U\left(\int_0^z \frac{ds}{L^2(s)}, \frac{\vec{r}}{L(z)}\right) \exp\left[\frac{i r^2}{4FL(z)}\right], \quad L(z) = 1 + \frac{z}{F}, \quad F = -\frac{a_s^2}{2C_s}.$$

Therefore, in Fig. 3 it is enough to calculate only the curve for non-focused beam because any initial distributions with pre-focusing will give the same result. The only difference would be a change in the position of the focal point:

$\frac{1}{z_f^{(A)}} + \frac{1}{F} = \frac{1}{z_f^{(U)}}$, where the index A and U denotes the focal length for the fields A and U, respectively.

Developed above formalism (Eqs. 2-4) can be used to estimate the interval Δz (see Fig. 1) where field intensity $I(r, z)$ exceeds the inscription threshold I_{th} , $I(r, z) > I_{th}$:

$$\left(\frac{\Delta z}{2}\right)^2 = \frac{k^2 a_s^2}{[1+C_s^2 - \frac{P_{in}}{P_{cr}}]^2} \left[\frac{P_{in}}{P_{cr}} \left[r_{cr}^2 \left(1+C_s^2 - \frac{P_{in}}{P_{cr}} \right) + a_s^2 \right] - a_s^2 \right]$$

in the limit of a tight focusing ($P_{in}/P_{cr} \ll 1+C_s^2$) this yields

$$\Delta z = 2k a_{\min_lin} \left[\frac{P_{in}}{P_{cr}} (r_{cr}^2 + a_{\min_lin}^2) - a_{\min_lin}^2 \right]^{1/2}, \quad a_{\min_lin}^2 = \frac{a_s^2}{1+C_s^2}.$$

This formula provides explains why the “NLSE stage” of the nonlinear beam dynamics (interval in z where beam propagation is well described by the NLS equation, or in other terms — the interval where energy is constant in Fig. 1) becomes shorter with growing input power. Namely the NLSE-evolution distance is given by:

$$z_{diss} = z_{\min_NL} - \Delta z/2 = \frac{k a_s^2 C_s}{[1+C_s^2 - P_{in}/P_{cr}]} - k a_s \left[\frac{P_{in}}{P_{cr}} \left(r_{cr}^2 + \frac{a_s^2}{1+C_s^2} \right) - \frac{a_s^2}{1+C_s^2} \right]^{1/2}.$$

It is instructive to re-write the results given by Eq. 2 in terms commonly used in experiments — numerical aperture NA, the focal length f , and the distance from the lens to the surface. We use here the commonly adopted definition of the beam radius, as the width at which the beam irradiance (intensity) has fallen to $1/e^2$ (13.5%) of its peak, or axial, value. Using the notations

introduced above, the beam radius on the surface reads: $2a_s^2 = \left(\frac{\lambda}{\pi NA}\right)^2 (1-NA^2) + \frac{NA^2(f-d)^2}{1-NA^2}$,

and the evolution of the RMS width is given by Eq. (2) where:

$$R_{\min_G}^2 = \frac{\lambda_0^2}{2\pi^2} \times \frac{1-NA^2}{NA^2} \times \frac{1-P(t)/P_{cr}}{1-P(t)/[P_{cr}(1+\frac{\pi^2(f-d)^2}{\lambda_0^2}(\frac{NA^2}{1-NA^2})^2)]},$$

$$z_{\min_G} = \frac{n_0 \times (f-d)}{1-P(t)/[P_{cr}(1+\frac{\pi^2(f-d)^2}{\lambda_0^2}(\frac{NA^2}{1-NA^2})^2)]}, \quad Z_{R_G}^2 = \frac{2R_{\min_G}^2 \times n_0^2 \times \frac{1-NA^2}{NA^2}}{1-P(t)/[P_{cr}(1+\frac{\pi^2(f-d)^2}{\lambda_0^2}(\frac{NA^2}{1-NA^2})^2)]}.$$

One can quantify to what extent the Kerr nonlinearity relaxes the requirements on the beam pre-focusing provided by linear lenses. Physically this means that diffraction is partially compensated by nonlinearity, therefore, the same focusing of the initial beam can be done by lens with smaller numerical aperture. It can be easily derived from the above formulae that in the case of a tight focusing, to achieve the same minimal beam width (that requires in the linear regime lens with numerical aperture NA_{linear}) in the nonlinear sub-critical regime, one can use lens with the numerical aperture NA_{NL} (index NL here indicates that nonlinear

propagation contributes to focusing): $NA_{NL}^2 = \frac{NA_{linear}^2 \times (1-P_{in}/P_{cr})}{1-NA_{linear}^2 \times P_{in}/P_{cr}}$. The dependence of

NA_{NL} on NA_{linear} is shown in Fig. 5 for several input powers (normalized to critical power).

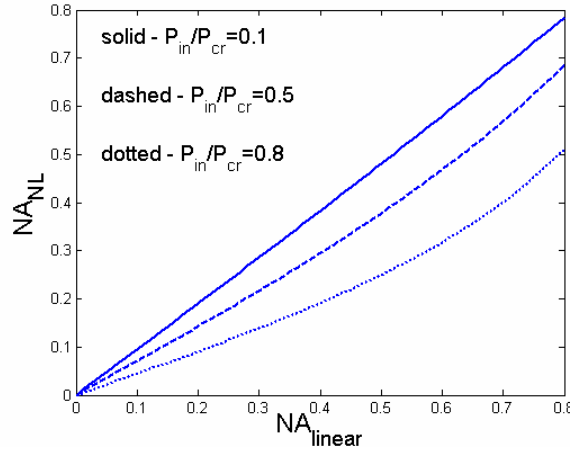


Fig. 5. Numerical aperture NA in the nonlinear regime vs numerical aperture of the linear focusing required to produce the same minimal beam size in the focal point for three values of the input power: 0.1, 0.5 and 0.8 (measured in critical power).

Note also that in the limit of a tight pre-focusing ($C_s^2 \gg 1$) the necessary condition of reaching inscription threshold can be written as (compare with [11]):

$$(5) \quad P_{in} = \frac{E_{in}}{\tau\sqrt{\pi}} = P_{th} = \frac{P_{cr} I_{th}}{I_{th} + 2\pi P_{cr} NA^2 / [\lambda_0^2 (1-NA^2)]}$$

Dependence of the normalized threshold energy E_{th} required for producing permanent structural change on the numerical aperture NA and the critical area $S_{cr} = P_{cr}/I_{th}$ defined above can be re-written as:

$$\frac{E_{th}}{P_{cr} \tau \sqrt{\pi}} = \frac{1}{1 + 2\pi \frac{NA^2}{1 - NA^2} \frac{S_{cr}}{\lambda_0^2}}.$$

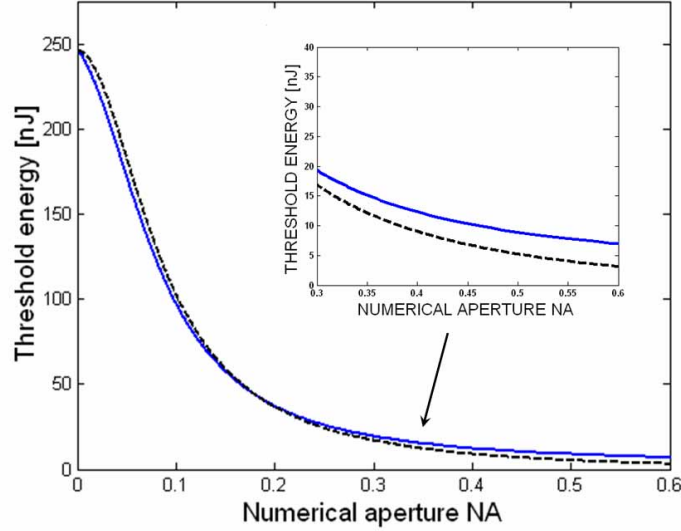


Fig. 6. Dependence of the inscription threshold energy required to produce irreversible change of the refractive index on the numerical aperture of a focusing lens using Gaussian pulse with FWHM = 100 fs. Solid line — Eq. 4, dashed line – approximation (5) effectively used in [11]. Inset shows the interval of NA from 0.3 to 0.6.

Note that though approximation given by Eq. (5) works rather well, more accurate description given by Eq. (4) still could of importance or some applications. As it was pointed out in [11], the dependence of the inscription threshold energy on the numerical aperture and self-focusing critical power shown in Fig. 6 can be used for determination of both P_{cr} and I_{th} . Therefore, maximum accurate description of this dependence at the pulse powers close to the critical power is an important issue.

3.2. Basics of the sub-critical focusing of the ring-shaped beams

Next we briefly discuss how the developed approach can be applied to laser beams having arbitrary initial shape, considering as a particular example a ring-shaped input field:

$A(r,0,t) = \sqrt{\frac{E_{in}}{\pi \sqrt{\pi} \tau a_s^{2+2m} m!}} r^m \exp\left[-\frac{(1+iC_s)r^2}{2a_s^2} - \frac{t^2}{2\tau^2}\right]$. In this case evolution of the RMS beam width can be presented in a form similar to Eq. 2:

$$R^2(z,t) = R_{\min_NL_m}^2 \left(1 + \frac{(z - z_{\min_m})^2}{Z_{R_NL_m}^2}\right),$$

$$R_{\min_NL_m}^2 = \frac{a_s^2(m+1)[1 - \frac{P(t)}{P_{cr_m}}]}{1 + (m+1)C_s^2 - \frac{P(t)}{P_{cr_m}}}, \quad Z_{R_NL_m}^2 = \frac{k^2 a_s^4(m+1)[1 - \frac{P(t)}{P_{cr_m}}]}{[1 + (m+1)C_s^2 - \frac{P(t)}{P_{cr_m}}]^2},$$

$$z_{\min} = \frac{k a_s^2 C_s(m+1)}{[1 + (m+1)C_s^2 - \frac{P(t)}{P_{cr_m}}]}, \quad P_{cr_m} = \frac{\lambda_0^2}{2\pi n_2 n_0} \times 2^{2m} (m!)^2 / (2m)!.$$

As expected, the critical power P_{cr_m} for the ring is higher by a factor of $2^{2m}(m!)^2/(2m)!$ compared to that for the normal Gaussian beams ($m=0$) (see e.g. [20]): $P_{cr_1} = 2P_{cr_G}$; $P_{cr_2} = 8P_{cr_G}/3$; $P_{cr_3} = 16P_{cr_G}/5$. Application of ring-structured beams can be used to create higher local field intensity yet, remaining in the sub-critical regime by delaying self-focusing that would otherwise immediately occur for single-humped beam profiles. Figure 7 compares evolution of field intensities (normalized by the inscription threshold intensity) for the initial Gaussian beam (left) and for a beam with ring distribution ($m = 1$, right picture) with the same other initial parameters: $P_m/P_{cr_G} = 0.5$ and pre-focusing parameter $C_s = 50$. It is seen that, indeed, a ring-shaped beam could be useful and efficient for creating higher local intensity (that is critical for inscription) using the same input power. We would like to stress that we do not aim here to make a fair comparison, because the nonlinear evolution of the ring beam is very different compared to that one with the Gaussian input spatial distribution. Therefore, a fair comparison of ring and Gaussian beams applied to inscription should include more accurate analysis of the impact of the pre-focusing conditions and input powers scaling and will be presented elsewhere. Our goal in this section is rather to attract attention to new opportunities offered by using non-Gaussian laser beams in the sub-critical inscription.

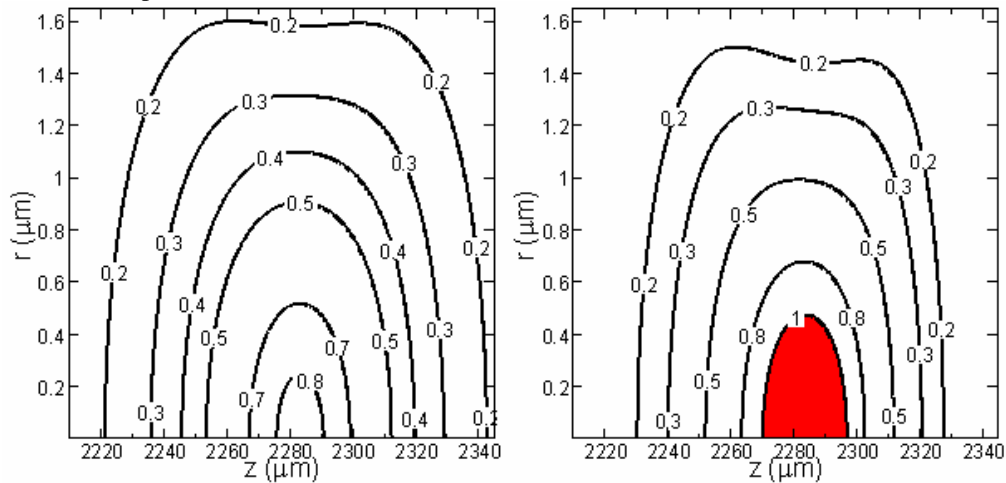


Fig. 7. Isolines of the normalized intensity $I(r, z)/I_{th}$ for initial Gaussian beam (left) and ring beam with $m=1$ (right); both with the input power $P_m/P_{cr} = 0.54$ and pre-focusing parameter $C_s = 50$. The area with $I(r, z) \geq I_{th}$ is shown by red.

4. Conclusions

We have examined theory of sub-critical regime of fs laser inscription in dielectric materials. Nonlinear modification of the widely used linear diffraction theory is presented. Simple nonlinear semi-analytical expression for the input beam power and spatial focusing parameter (numerical aperture) required to achieve the inscription threshold are derived. It is proposed to use non-Gaussian laser beams having larger self-focusing threshold for better controlled fs inscription at higher powers. Delayed self-focusing at high powers using non-Gaussian beams can be potentially useful for inscription of structures for telecommunication applications requiring waveguides on the scale of several microns.